

## Outbreak Reports

## Infection Tracing and Virus Genomic Analysis of Two Cases of Human Infection with Avian Influenza A(H5N6) — Fujian Province, China, April–May 2024

Yanhua Zhang<sup>1</sup>; Jingjing Wu<sup>1</sup>; Qi Lin<sup>1</sup>; Jianming Ou<sup>1</sup>; Xiaoqi Qi<sup>1</sup>; Youxian Zheng<sup>2</sup>; Fengping Li<sup>2</sup>; Yuwei Weng<sup>1,†</sup>

### Summary

#### What is known about this topic?

Global human cases of zoonotic influenza A(H5N6) have increased significantly in recent years, primarily due to widespread circulation of clade 2.3.4.4b virus since 2020. Concurrent with this trend, sporadic human infections with clade 2.3.4.4h H5N6 avian influenza virus continue to occur. The high mortality rate associated with H5N6 virus infections has emerged as a critical public health concern.

#### What is added by this report?

Through comprehensive field epidemiological investigations and laboratory analyses, we identified the infection sources for these cases and conclusively ruled out human-to-human transmission. Genetic analyses revealed that while the virus maintains its avian host tropism, it has acquired mutations that may enhance human receptor binding affinity, viral replication capacity, pathogenicity, and neuraminidase inhibitor resistance.

#### What are the implications for public health practice?

The ongoing viral mutations increase the potential for H5 subtype avian influenza viruses to overcome species barriers and cause human epidemics. Enhanced surveillance strategies incorporating advanced technologies, such as metagenomic sequencing, are essential for early risk detection and management. Special attention should be directed toward cancer patients and immunocompromised individuals, who demonstrate increased susceptibility to avian influenza virus infections and require targeted prevention and control measures.

In recent years, avian influenza viruses, particularly those of the H5 subtype, have emerged as significant public health concerns. While these viruses primarily circulate in wild birds and domestic poultry with sporadic human infections, they possess pandemic

potential. Although sustained human-to-human transmission of H5 subtypes has not been documented, the reporting of two human H5N6 avian influenza cases in Quanzhou City within a one-month period warranted immediate investigation as a potential infection cluster. This study employed integrated field epidemiological investigations and genetic analyses to trace the infection sources of the 2.3.4.4h clade H5 subtype avian influenza virus, aiming to identify potential risks and establish evidence-based prevention and control strategies.

## INVESTIGATION AND RESULTS

### Tracing the Source of Infection

From April to May 2024, two cases of human H5N6 avian influenza infection were reported in Quanzhou City, Fujian Province, China. Following case identification, local health authorities and CDC teams immediately initiated comprehensive epidemiological investigations, laboratory analyses, and control measures.

Case A, a previously healthy 52-year-old female from Quangang District, developed symptoms following exposure to heavy cold rain on April 13, 2024. Laboratory sampling on April 21 yielded H5N6-positive results on April 23, and the patient succumbed to the infection on April 30. The patient worked at a salt field within 2 kilometers of her residence. Family members reported that she had remained within Quangang District with no travel history in the 10 days preceding symptom onset. She maintained a small poultry flock in a shed 50 meters from her home, where several poultry had recently fallen ill. Eight days before symptom onset, she had slaughtered and consumed these diseased poultry. Following symptom onset, she sought medical attention sequentially at a village clinic, township health center, and hospital.

Case B, a 40-year-old male from Luojiang District with nasopharyngeal cancer and pulmonary metastases,

developed symptoms on May 8, 2024. He tested positive on May 14 and died that evening. The patient, who primarily convalesced at home due to his cancer condition, resided with his parents who maintained a poultry shed west of their residence. While he had no direct contact with poultry or live poultry markets, his village featured widespread household poultry keeping, with reports of poultry illness and mortality approximately one month prior. His only potential exposure occurred during occasional walks along village paths adjacent to these poultry sheds.

The residences of Cases A and B were separated by approximately 27 kilometers. Although both patients received treatment at the same hospital, no epidemiological links were identified during their hospital stays, and no other direct or indirect connections were established. The spatio-temporal relationships between the two cases are illustrated in [Figure 1](#).

During the outbreak response, surveillance identified 21 close contacts of Case A and 6 close contacts of Case B. All contacts underwent 10 days of medical observation with negative nucleic acid test results before release, confirming the absence of secondary infections.

Environmental sampling was conducted to identify potential infection sources for both cases. Following a risk-based sampling strategy and site disinfection protocols, we initially collected samples from the patients' outdoor poultry sheds and indoor environments, followed by sampling of neighboring sheds and nearby live poultry markets. For Case A, all 84 collected samples tested negative. For Case B, after initial negative results from 15 environmental samples, we expanded sampling to include the patient's poultry shed (10 samples), neighboring poultry sheds (110 samples), and local live poultry markets (92 samples). While the patient's shed remained negative, positive results were detected in neighboring sheds (2.73%, 3/110) and live poultry markets (5.43%, 5/92). Detailed positive sample information is presented in [Supplementary Table S1](#) (available at <https://weekly.chinacdc.cn/>).

Nucleic acid-positive samples underwent next-generation sequencing (NGS) using the MiniSeq™ DX-CN platform (Illumina, San Diego, USA). Raw data processing and assembly were performed using CLC Genomics Workbench 23.0 (Qiagen, Hilden, Germany). High-quality genomic sequences were obtained from two case samples and six of eight environmental samples, with A/Environment/Fujian/02-Env04/2024(H5N6) and A/Environment/

Fujian/02-Env06/2024(H5N6) yielding insufficient quality. The virus strains were designated as A/Fujian/01/2024(H5N6) (FJ01) from Case A and A/Fujian/02/2024(H5N6) (FJ02) from Case B. Pairwise nucleotide sequence identity analysis was conducted using MegAlign software (version 7.1.0, DNASTAR, Inc., USA), with results presented in [Table 1](#).

Sequence analysis revealed partial genetic divergence between Cases A and B, with 100% identity observed only in the matrix protein (MP) and nonstructural protein (NS) segments. Notably, Case B's viral sequences showed complete identity with those from neighboring poultry shed Z but differed from samples collected from other nearby sheds and markets. Significantly, shed Z was positioned on an elevated terrain approximately 50 meters from the patient's residence and 8 meters from his regular walking path.

## Genomic Analysis of Viruses

Comparative genomic analysis was performed on the eight segments from the FJ01 and FJ02 strains using the Basic Local Alignment Search Tool (BLAST) against both the National Center for Biotechnology Information (NCBI, USA) and Global Initiative on Sharing All Influenza Data (GISAID) databases. The analysis revealed that the PB2, PB1, PA, and HA segments of both strains showed highest sequence homology with A/Guangdong/Igf/2021(H5N6), A/duck/Hunan/S40199/2021(H5N6), A/Neogale vison/China/FD/NV/SD/L4/2021(H5N6), and A/Rattus norvegicus/China/FS21/2021, respectively. The remaining segments (NP, NA, MP, and NS) demonstrated highest similarity to A/Guangdong/1/2021(H5N6). Detailed BLAST results are presented in [Supplementary Table S2](#) (available at <https://weekly.chinacdc.cn/>).

Sequence alignment was conducted on the hemagglutinin (HA) gene segments of the FJ01 and FJ02 strains using MAFFT version 7 (<https://mafft.cbrc.jp/alignment/server/>). The phylogenetic analysis was performed using MEGA software (version 7.0.26, Pennsylvania State University, USA), employing the Maximum Likelihood method with the Tamura-Nei model and 1,000 bootstrap replicates to ensure statistical robustness. Reference sequences were obtained from the GISAID database. Both HA genes were definitively classified within clade 2.3.4.4h, as illustrated in [Supplementary Figure S1](#) (available at <https://weekly.chinacdc.cn/>).

Comprehensive molecular characterization of the

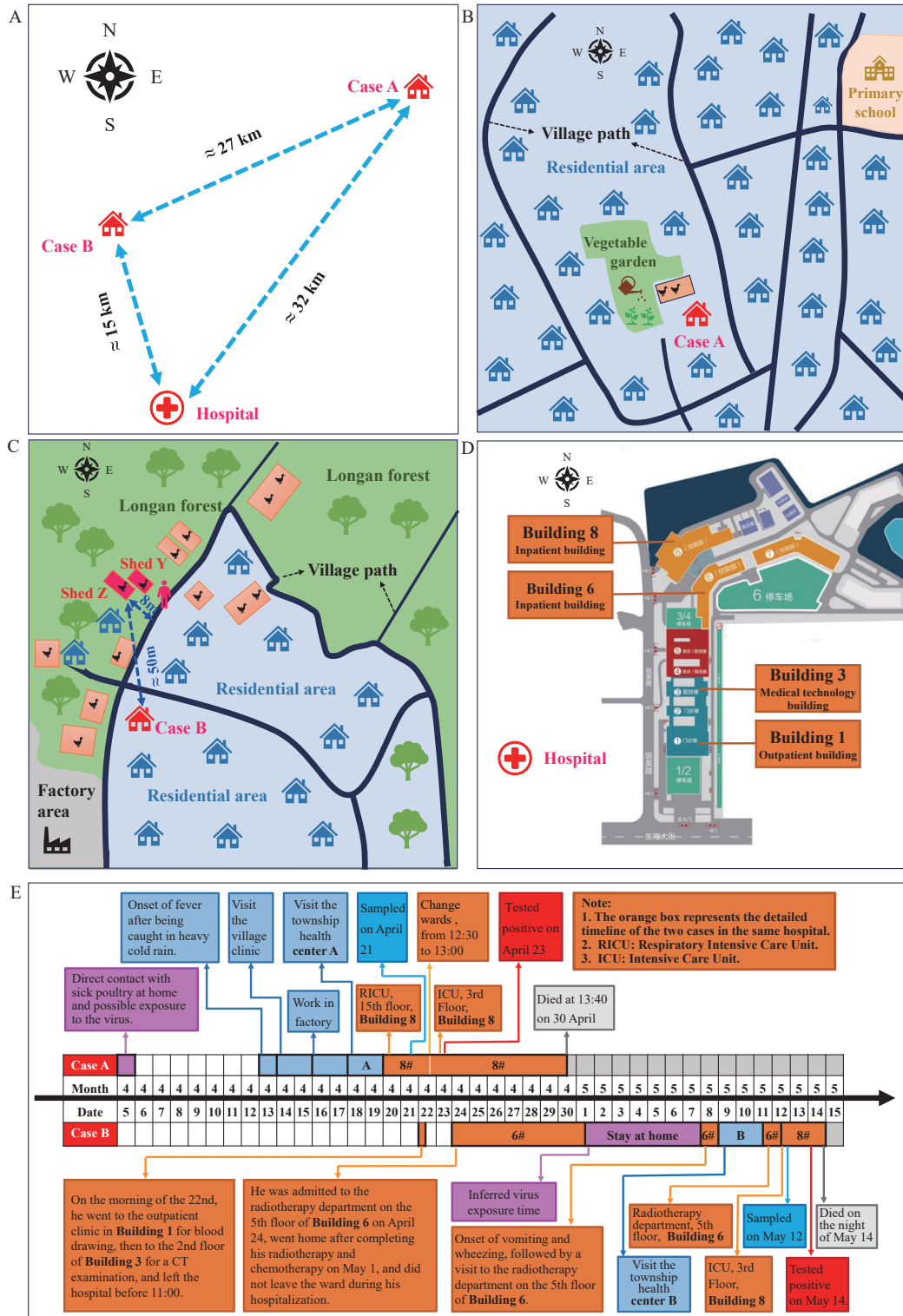


FIGURE 1. The spatio-temporal relationship analysis of the two cases. (A) Spatial distribution of cases and hospital locations; (B) Case A's residence (red house) and associated poultry shed (light orange box); (C) Case B's residence (red house) and sampled surrounding poultry sheds, with virus-positive sheds indicated in red; (D) Hospital layout diagram showing areas where both Case A and Case B received treatment; (E) Post-onset activity timeline for both cases, with the orange box highlighting their concurrent hospital stays. Note: For (C) The patient's family poultry shed was situated west of the residence.

TABLE 1. Nucleotide sequence identity matrix comparing case samples and environmental isolates.

Virus strains	The percent identity between FJ02 and other strains							
	PB2	PB1	PA	HA	NP	NA	MP	NS
FJ01	99.92	99.91	99.91	99.76	99.93	99.71	100.00	100.00
A/Environment/Fujian/02-Env01/2024(H5N6)	99.98	100.00	99.95	100.00	99.93	99.93	100.00	99.88
A/Environment/Fujian/02-Env02/2024(H5N6)	100.00	100.00	100.00	100.00	100.00	100.00	100.00	100.00
A/Environment/Fujian/02-Env03/2024(H5N6)	100.00	100.00	100.00	100.00	100.00	100.00	100.00	100.00
A/Environment/Fujian/02-Env04/2024(H5N6)	94.26	86.60	85.85	–	89.44	86.04	96.04	89.64
A/Environment/Fujian/02-Env05/2024(H5N6)	99.89	99.87	89.68	99.82	100.00	99.85	99.96	99.88
A/Environment/Fujian/02-Env06/2024(H5N6)	96.12	94.99	99.91	99.17	94.77	98.01	97.55	95.29
A/Environment/Fujian/02-Env07/2024(H5N6)	99.38	98.75	98.68	99.29	98.92	97.86	99.49	98.30
A/Environment/Fujian/02-Env08/2024(H5N6)	99.41	98.80	98.73	99.29	99.06	98.01	99.49	98.30

Note: “–” means that the sequence quality is too low (less than 50% coverage) to be analyzed.

FJ01 and FJ02 strains was conducted through sequence analysis. The HA and NA protein coding followed H3N2 numbering conventions. Complete results are presented in Table 2.

## PUBLIC HEALTH RESPONSE

Local health authorities and CDC teams implemented comprehensive public health measures in response to the outbreak, including: 1) enhanced 2-week surveillance of influenza-like illnesses (ILI) in outpatient settings and severe acute respiratory infections (SARI) in hospitalized patients, with pre-screening and triage protocols to prevent nosocomial transmission; 2) emergency 2-week citywide environmental monitoring of poultry-related environments; 3) immediate disinfection of outbreak sites with subsequent effectiveness evaluation; 4) coordinated prevention efforts with the Agriculture Department for at-risk poultry culling and free-range poultry immunization enhancement, and collaboration with the Market Regulation Authority to implement “three ones” measures in live poultry markets (daily cleaning, weekly disinfection, and monthly closure); and 5) strategic risk communication, health education, and public information dissemination.

The implemented control measures proved effective, with no new infections reported and all close contacts remaining uninfected as of May 29, leading to the formal declaration of the outbreak’s conclusion.

## DISCUSSION

Comprehensive analysis of epidemiological and laboratory data demonstrated that cases A and B were

independent events with no epidemiological links. Medical observation of all close contacts revealed no signs of infection, providing strong evidence against human-to-human transmission in both cases.

Environmental investigation plays a crucial role in tracing avian influenza virus infections. Although both cases were associated with poultry illness or mortality prior to symptom onset, initial environmental sampling from the patients’ poultry sheds yielded negative results. This unexpected outcome can be attributed to two factors: the rapid disposal of diseased poultry before patient illness onset, which eliminated environmental viral evidence, and the implementation of thorough disinfection measures by families or health authorities prior to sampling. Nevertheless, viral genetic sequencing analysis of samples from surrounding poultry sheds near Case B provided definitive evidence for outbreak source identification.

The transmission routes differed between the two cases. Case A’s infection likely resulted from direct contact with diseased poultry, while Case B, who had no direct poultry exposure, suggested an alternative transmission pathway. Genetic analysis revealed 100% nucleotide sequence identity between Case B’s virus and samples from poultry shed Z, while distinct genetic differences were observed in viruses from shed Y and local live poultry markets. This evidence strongly indicates shed Z as Case B’s infection source. Although the viruses from both cases showed high sequence similarity, they were not identical, ruling out direct transmission between cases. The absence of infection among close contacts further confirms the lack of human-to-human transmission.

The location of poultry shed Z, approximately 8 meters from Case B’s regular walking route, suggests

TABLE 2. Key molecular markers associated with influenza virus pathogenicity.

Genes	Molecular markers	FJ01	FJ02	Phenotypic effect
HA	Cleavage site <sup>*</sup>	RERRRKR↓GLF		Shows multiple basic amino acids and high pathogenicity to chickens.
	S127P (1)	S	S	Increases virus binding to $\alpha$ 2–6 sialic acids ( $\alpha$ 2–6 SA).
	<b>S137A (1)</b>	<b>A</b>	<b>A</b>	<b>Increases virus binding to <math>\alpha</math>2–6 SA.</b>
	G143R <sup>*</sup>	G	G	Increases virus binding to $\alpha$ 2–6 SA.
	<b>I155T (2)</b>	<b>T</b>	<b>T</b>	<b>Increases virus binding to <math>\alpha</math>2–6 SA.</b>
	N158D <sup>*</sup>	N	N	Increases virus binding to $\alpha$ 2–6 SA, and increases airborne transmissibility.
	<b>T160A<sup>*</sup></b>	<b>A</b>	<b>A</b>	<b>Increases virus binding to both <math>\alpha</math>2,3-SA and <math>\alpha</math>2,6-SA, and increase airborne transmissibility.</b>
	V214I <sup>*</sup>	V	V	Increases virus binding to $\alpha$ 2–6 SA.
	N224K <sup>*</sup>	N	N	Increases virus binding to $\alpha$ 2–6 SA, and increases airborne transmissibility.
	Q226L <sup>*</sup>	Q	Q	Increases virus binding to $\alpha$ 2–6 SA.
	S227N <sup>*</sup>	R	S	Increases virus binding to $\alpha$ 2–6 SA.
G228S <sup>*</sup>	G	G	Increases virus binding to $\alpha$ 2–6 SA.	
NA	<b>58-68 Delete (3)</b>	<b>Delete</b>	<b>Delete</b>	<b>Associated with increased viral virulence in mammals.</b>
	E119V (4)	E	E	Shows different degrees of neuraminidase inhibitor resistance.
	<b>D198N (5)</b>	<b>N</b>	<b>N</b>	<b>Shows neuraminidase inhibitor resistance.</b>
	H274Y <sup>**</sup>	H	H	Shows neuraminidase inhibitor resistance.
PB2	<b>K389R (6)</b>	<b>R</b>	<b>R</b>	<b>Enhances growth capacity in human and mammalian cells.</b>
	Q591K <sup>**</sup>	Q	Q	Increases pathogenicity in mice.
	E627K <sup>**</sup>	E	E	Associated with mammalian adaptation, increases virus replication in mammalian cells, increases virulence in mice, increases transmissibility in ferrets, determinant of cold sensitivity.
	D701N <sup>**</sup>	D	D	Associated with mammalian adaptation, increases virus replication in mammalian cells, improves binding of PB2 to importin protein in mammalian cells.
PB1	<b>D3V<sup>*</sup></b>	<b>V</b>	<b>V</b>	<b>Enhances viral polymerase activity.</b>
	H99Y <sup>*</sup>	H	H	Increases viral polymerase activity, and associated with mammalian adaptation.
	M317I <sup>***</sup>	M	M	Increased pathogenicity in mice.
	<b>L473V<sup>***</sup></b>	<b>V</b>	<b>V</b>	<b>Maintains efficient viral replication.</b>
	<b>D622G<sup>*</sup></b>	<b>G</b>	<b>G</b>	<b>Enhances viral polymerase activity and virulence in mice.</b>
PA	I38T/L (7)	I	I	Reduces the susceptibility of polymerase acidic (PA) endonuclease inhibitor.
	T97I <sup>***</sup>	T	T	Associated with mammalian adaptation.
	K142Q <sup>***</sup>	K	K	Enhances replication and pathogenesis in mice when combined with PB2 627K, associated with mammalian adaptation.
	<b>K615R<sup>***</sup></b>	<b>R</b>	<b>R</b>	<b>Increases viral virulence in mammals when combined with NP N319K.</b>
NS1	<b>P42S<sup>*</sup></b>	<b>S</b>	<b>S</b>	<b>Increases viral virulence in mice by preventing the dsRNA-mediated activation of the NF-<math>\kappa</math>B and IRF – 3 pathways.</b>
	P212S <sup>**</sup>	P	P	Promotes viral replication in mice.
	D92E <sup>**</sup>	D	D	Increased virulence and/or cytokine resistance.
NP	N319K <sup>***</sup>	N	N	Increases viral virulence in mammals when combined with PA K615R.
M2	L26F <sup>**</sup>	L	L	Shows antiviral amantadine resistance.
	V27A <sup>**</sup>	V	V	Shows antiviral amantadine resistance.
	A30T <sup>**</sup>	A	A	Shows antiviral amantadine resistance.
	S31N <sup>**</sup>	S	S	Shows antiviral amantadine resistance.
	G34E <sup>**</sup>	G	G	Shows antiviral amantadine resistance.

Note: HA and NA mutation sites follow H3N2 numbering conventions. Bold text indicates that the mutations have occurred in the viruses reported in this study.

Abbreviation: HA=Hemagglutinin; NA=neuraminidase.

\* Data derived from reference (8);

\*\* Data derived from reference (9);

\*\*\* Data derived from reference (10).

potential aerosol transmission over this distance. Notably, both cases exhibited compromised immune status: Case A experienced heavy rain exposure before illness onset, while Case B had nasopharyngeal cancer with ongoing chemotherapy and radiotherapy. The absence of symptoms among family members despite potential viral exposure suggests that immunocompromised status may represent a significant risk factor for H5N6 avian influenza virus infection in humans.

While genomic analysis revealed no significant recombination compared to recent H5N6 viruses, several concerning features were identified, including a highly pathogenic HA protein cleavage site and mutations associated with increased virulence, human infection potential, enhanced viral replication, and possible neuraminidase inhibitor resistance. The ongoing H5N1 outbreak in mammals in the United States heightens concerns about potential cross-species transmission and human epidemic risk. Although sustained human-to-human transmission of H5 subtype viruses remains undocumented, these findings underscore the critical importance of enhanced surveillance and robust pandemic preparedness measures.

**Conflicts of interest:** No conflicts of interest.

**Acknowledgments:** The staff from the Quanzhou Municipal Center for Disease Control and Prevention, the Second Affiliated Hospital of Fujian Medical University, Quangang District Center for Disease Control and Prevention, and Luojiang District Center for Disease Control and Prevention.

**Funding:** Supported by the Fujian Natural Science Foundation (2021J01351) and the Major Scientific Research Program for Young and Middle-aged Health Professionals of Fujian Province, China (Grant No.2021ZQNZD006).

doi: [10.46234/ccdcw2024.274](https://doi.org/10.46234/ccdcw2024.274)

\* Corresponding author: Yuwei Weng, [wengyuwei@fjcdc.com.cn](mailto:wengyuwei@fjcdc.com.cn).

<sup>1</sup> Fujian Provincial Center for Disease Control and Prevention, Fujian Provincial Key Laboratory of Zoonosis Research, Fuzhou City, Fujian Province, China; <sup>2</sup> Quanzhou Municipal Center for Disease Control and Prevention, Quanzhou City, Fujian Province, China.

Copyright © 2025 by Chinese Center for Disease Control and Prevention. All content is distributed under a Creative Commons Attribution Non Commercial License 4.0 (CC BY-NC).

Submitted: September 24, 2024

Accepted: November 25, 2024

Issued: December 18, 2024

## REFERENCES

1. Cao L, Liu YH, Li KB, Lu JY, Lu EJ, Chen YY, et al. Epidemiological and genetic characteristics of H5 subtype avian influenza virus in Guangzhou, 2014-2019. *Chin J Epidemiol* 2020;41(7):1115 - 20. <https://doi.org/10.3760/cma.j.cn112338-20190730-00565>.
2. He DL, Wang FF, Zhao LM, Jiang XN, Zhang S, Wei F, et al. Epidemiological investigation of infectious diseases in geese on mainland China during 2018-2021. *Transbound Emerg Dis* 2022;69(6):3419 - 32. <https://doi.org/10.1111/tbed.14699>.
3. He ZL, Wang X, Lin Y, Feng SY, Huang XY, Zhao LX, et al. Genetic characteristics of waterfowl-origin H5N6 highly pathogenic avian influenza viruses and their pathogenesis in ducks and chickens. *Front Microbiol* 2023;14:1211355. <https://doi.org/10.3389/fmicb.2023.1211355>.
4. Bialy D, Shelton H. Functional neuraminidase inhibitor resistance motifs in avian influenza A(H5Nx) viruses. *Antiviral Res* 2020;182:104886. <https://doi.org/10.1016/j.antiviral.2020.104886>.
5. Hossain MG, Akter S, Dhole P, Saha S, Kazi T, Majbauddin A, et al. Analysis of the genetic diversity associated with the drug resistance and pathogenicity of influenza a virus isolated in Bangladesh from 2002 to 2019. *Front Microbiol* 2021;12:735305. <https://doi.org/10.3389/fmicb.2021.735305>.
6. Bi FY, Jiang LL, Huang LH, Wei JG, Pan XW, Ju Y, et al. Genetic characterization of two human cases infected with the avian influenza a (H5N6) viruses - Guangxi Zhuang autonomous region, China, 2021. *China CDC Wkly* 2021;3(44):923 - 8. <https://doi.org/10.46234/ccdcw2021.199>.
7. Hickerson BT, Petrovskaya SN, Dickensheets H, Donnelly RP, Ince WL, Ilyushina NA. Impact of Baloxavir resistance-associated substitutions on influenza virus growth and drug susceptibility. *J Virol* 2023;97(7):e00154 - 23. <https://doi.org/10.1128/jvi.00154-23>.
8. Liang YY. Pathogenicity and virulence of influenza. *Virulence* 2023;14(1):2223057. <https://doi.org/10.1080/21505594.2023.2223057>.
9. Xiao CK, Xu JN, Lan Y, Huang ZP, Zhou LJ, Guo YX, et al. Five independent cases of human infection with avian influenza H5N6 - Sichuan Province, China, 2021. *China CDC Wkly* 2021;3(36):751 - 6. <https://doi.org/10.46234/ccdcw2021.187>.
10. Griffin EF, Tompkins SM. Fitness determinants of influenza a viruses. *Viruses* 2023;15(9):1959. <https://doi.org/10.3390/v15091959>.

## SUPPLEMENTARY MATERIAL

SUPPLEMENTARY TABLE S1. Information on nucleic acid-positive samples and corresponding virus strain nomenclature.

Virus strains	GISAID Accession No.	Sample source	Sample type
A/Fujian/01/2024(H5N6)	EPI_ISL_19132453	Case A	Bronchoalveolar lavage fluid
A/Fujian/02/2024(H5N6)	EPI_ISL_19145644	Case B	Oropharyngeal
A/Environment/Fujian/02-Env01/2024(H5N6)	/	Shed Y	Poultry drinking water
A/Environment/Fujian/02-Env02/2024(H5N6)	/	Shed Z	Poultry drinking water
A/Environment/Fujian/02-Env03/2024(H5N6)	/	Shed Z	Poultry drinking water
A/Environment/Fujian/02-Env04/2024(H5N6)	/	LPM	Poultry drinking water
A/Environment/Fujian/02-Env05/2024(H5N6)	/	LPM	Poultry drinking water
A/Environment/Fujian/02-Env06/2024(H5N6)	/	LPM	Poultry drinking water
A/Environment/Fujian/02-Env07/2024(H5N6)	/	LPM	Poultry drinking water
A/Environment/Fujian/02-Env08/2024(H5N6)	/	LPM	Cutting board swab

Note: Shed Y was located approximately 50 meters from Case B's residence, with Shed Z situated adjacent to Shed Y. LPM refers to live poultry markets in Case B's vicinity.

SUPPLEMENTARY TABLE S2. Similarity analysis of viral genome segments using BLAST.

Virus	Segment and length (bp)	Strain with the highest similarity (accession ID, percent identity)	
		NCBI database	GISAID database
FJ01	PB2:2250	A/Guangdong/lgf/2021(H5N6) (OL519558.1, 98.68%)	A/Guangdong/lgf/2021 (H5N6) (EPI2255274, 98.68%)
FJ01	PB1:2239	A/duck/Guangxi/293D21/2017(H1N2) (MH667662.1, 96.44%)	A/duck/Hunan/S40199/2021(H5N6) (H5N6) (EPI1997200, 98.42%)
FJ01	PA: 2131	A/Guangdong/1/2021(H5N6) (OK284448.1, 99.02%)	A/Neogale vison/ China/FD/NV/SD/L4/2021 (H5N6) (EPI3351954, 99.07%)
FJ01	HA: 1725	A/Rattus norvegicus/China/FS21/2021 (H5N6) (OQ291577.1, 97.24%)	A/Rattus norvegicus/China/FS21/2021 (H5N6) (EPI2394816, 97.24%)
FJ01	NP: 1551	A/Guangdong/1/2021(H5N6) (OK284449.1, 99.04%)	A/Guangdong/1/2021 (H5N6) (EPI2200687, 99.04%)
FJ01	NA: 1398	A/Guangdong/1/2021(H5N6) (OK284452.1, 98.04%)	A/Guangdong/1/2021 (H5N6) (EPI2200690, 98.04%)
FJ01	MP: 1021	A/Guangdong/1/2021(H5N6) (OK284450.1, 99.42%)	A/Bar-headed Goose/Tibet/XZQ17-1/2021 (H5N8) (EPI1949225, 99.42%)
FJ01	NS: 872	A/Guangdong/1/2021(H5N6) (OK284453.1, 97.98%)	A/Guangdong/1/2021 (H5N6) (EPI2200691, 97.98%)
FJ02	PB2: 2247	A/Guangdong/lgf/2021(H5N6) (OL519558.1, 98.55%)	A/Guangdong/lgf/2021 (H5N6) (EPI2255274, 98.55%)
FJ02	PB1: 2239	A/duck/Guangxi/293D21/2017(H1N2) (MH667662.1, 96.44%)	A/duck/Hunan/S40199/2021(H5N6) (EPI1997200, 98.42%)
FJ02	PA: 2133	A/Guangdong/1/2021(H5N6) (OK284448.1, 99.12%)	A/Neogale vison/China/FD/NV/SD/L4/2021 (H5N6) (EPI3351954, 99.16%)
FJ02	HA: 1725	A/Rattus norvegicus/China/FS21/2021(H5N6) (OQ291577.1, 97.24%)	A/Rattus norvegicus/China/FS21/2021 (H5N6) (EPI2394816, 97.24%)
FJ02	NP: 1552	A/Guangdong/1/2021(H5N6) (OK284449.1, 99.11%)	A/Guangdong/1/2021 (H5N6) (EPI2200687, 99.11%)
FJ02	NA: 1400	A/Guangdong/1/2021(H5N6) (OK284452.1, 98.18%)	A/Guangdong/1/2021 (H5N6) (EPI2200690, 98.18%)
FJ02	MP: 1021	A/Guangdong/1/2021(H5N6) (OK284450.1, 99.42%)	A/Bar-headed Goose/Tibet/XZQ17-1/2021 (H5N8) (EPI1949225, 99.42%)
FJ02	NS: 872	A/Guangdong/1/2021(H5N6) (OK284453.1, 97.98%)	A/Guangdong/1/2021 (H5N6) (EPI2200691, 97.98%)

Abbreviation: BLAST=basic local alignment search tool; NCBI=national center for biotechnology information (USA); GISAID=global initiative on sharing all influenza data.



SUPPLEMENTARY FIGURE S1. Phylogenetic analysis of H5 virus HA genes using the maximum likelihood method. Note: The phylogenetic tree encompasses major H5 clades (indicated at terminal nodes) and is rooted in the reference strain A/Goose/Guangdong/1/1996 (H5N1). The tree was constructed using 1,000 bootstrap replicates, with values shown above branches. Viral strains from this study are denoted by red spots (case A), red triangles (case B), and black triangles (environmental isolates). Abbreviation: HA=hemagglutinin.